



## Article

# High-Throughput Screening to Identify Inhibitors of *Plasmodium falciparum* Importin $\alpha$

Sujata B. Walunj<sup>1,2,3</sup>, Manisha M. Dias<sup>1</sup>, Chhaminder Kaur<sup>2</sup> , Kylie M. Wagstaff<sup>1</sup>, Vishakha Dey<sup>2</sup>, Caroline Hick<sup>4</sup>, Swati Patankar<sup>2,†</sup> and David A. Jans<sup>1,\*,†</sup> 

<sup>1</sup> Nuclear Signaling Laboratory, Department of Biochemistry and Molecular Biology, Monash Biomedicine Discovery Institute, Monash University, Clayton, VIC 3800, Australia; sujata.walunj@monash.edu (S.B.W.); manisha.treeby@monash.edu (M.M.D.); kylie.wagstaff@monash.edu (K.M.W.)

<sup>2</sup> Molecular Parasitology Laboratory, Department of Biosciences and Bioengineering, IIT Bombay, Powai, Mumbai 400076, India; chhaminder.kaur@iitb.ac.in (C.K.); vishakhadey@gmail.com (V.D.); patankar@iitb.ac.in (S.P.)

<sup>3</sup> IITB-Monash Research Academy, IIT Bombay, Mumbai 400076, India

<sup>4</sup> Monash Institute of Pharmaceutical Sciences, Monash University, Parkville, VIC 3052, Australia; caroline.hick@monash.edu

\* Correspondence: david.jans@monash.edu

† These authors contributed equally to this work.



**Citation:** Walunj, S.B.; Dias, M.M.; Kaur, C.; Wagstaff, K.M.; Dey, V.; Hick, C.; Patankar, S.; Jans, D.A. High-Throughput Screening to Identify Inhibitors of *Plasmodium falciparum* Importin  $\alpha$ . *Cells* **2022**, *11*, 1201. <https://doi.org/10.3390/cells11071201>

Academic Editors: Alberto Muñoz-Prieto, José Joaquín Cerón, Vladimir Mrljak and Lorena Franco-Martinez

Received: 5 March 2022

Accepted: 29 March 2022

Published: 2 April 2022

**Publisher's Note:** MDPI stays neutral with regard to jurisdictional claims in published maps and institutional affiliations.



**Copyright:** © 2022 by the authors. Licensee MDPI, Basel, Switzerland. This article is an open access article distributed under the terms and conditions of the Creative Commons Attribution (CC BY) license (<https://creativecommons.org/licenses/by/4.0/>).

**Abstract:** The global burden of malaria and toxoplasmosis has been limited by the use of efficacious anti-parasitic agents, however, emerging resistance in *Plasmodium* species and *Toxoplasma gondii* threatens disease control worldwide, implying that new agents/therapeutic targets are urgently needed. Nuclear localization signal (NLS)-dependent transport into the nucleus, mediated by members of the importin (IMP) superfamily of nuclear transporters, has shown potential as a target for intervention to limit viral infection. Here, we show for the first time that IMP $\alpha$  from *P. falciparum* and *T. gondii* have promise as targets for small molecule inhibitors. We use high-throughput screening to identify agents able to inhibit *P. falciparum* IMP $\alpha$  binding to a *P. falciparum* NLS, identifying a number of compounds that inhibit binding in the  $\mu$ M–nM range, through direct binding to *P. falciparum* IMP $\alpha$ , as shown in thermostability assays. Of these, BAY 11-7085 is shown to be a specific inhibitor of *P. falciparum* IMP $\alpha$ -NLS recognition. Importantly, a number of the inhibitors limited growth by both *P. falciparum* and *T. gondii*. The results strengthen the hypothesis that apicomplexan IMP $\alpha$  proteins have potential as therapeutic targets to aid in identifying novel agents for two important, yet neglected, parasitic diseases.

**Keywords:** *Plasmodium falciparum*; malaria; *Toxoplasma gondii*; toxoplasmosis; importins; nuclear import inhibitors

## 1. Introduction

Organisms from the phylum apicomplexa, such as *Plasmodium* spp., *Toxoplasma gondii*, *Cyclospora* spp., and *Cryptosporidium* spp., can cause severe disease in humans [1,2]. The World Health Organization (WHO) estimates close to 240 million malaria cases caused by *Plasmodium* spp. in 2020 [3], with >600,000 deaths, predominantly of children under the age of five. *T. gondii* chronically infects about one-third of the human population worldwide with the majority of infections being asymptomatic, however, infection of immunocompromised individuals (such as those suffering from autoimmune diseases syndrome—AIDS) can result in severe toxoplasmosis, whilst in the case of pregnant women, hydrocephaly/microcephaly can occur in new-born babies [4–6]. Emerging drug resistance to the current frontline chemotherapy is a major threat to the control of malaria and toxoplasmosis [6–8], with an accompanying urgent need for new drugs with novel mechanisms of action to control these diseases.

Signal-dependent transport into and out of the eukaryotic cell nucleus, mediated by members of the importin (IMP) superfamily of proteins, is central to processes such as cell differentiation, transformation, development, and infection and immunity [9–13]. In a classical nuclear import,  $\text{IMP}\alpha$  recruits  $\text{IMP}\beta 1$  through its  $\text{IMP}\beta$ -binding domain (IBB) and then binds to the nuclear localization signal (NLS) of cargo proteins to be subsequently imported into the nucleus [10,11,14]. In the absence of  $\text{IMP}\beta 1$ ,  $\text{IMP}\alpha$  is deemed to be “autoinhibited” with only low affinity for NLSs due to binding of its IBB in the NLS-binding pocket of  $\text{IMP}\alpha$  [15]; this is essential to facilitate cargo release in the nucleus [11,16] after  $\text{IMP}\beta 1$  is dissociated from the transport complex upon binding of the monomeric guanine nucleotide-binding protein Ran in its activated GTP-bound form [10,11,13]. Dysregulation of nucleocytoplasmic transport can impact a range of cellular processes [9,15,16], with the inhibition of nuclear transport holding great potential for therapeutic intervention [17–20].

IMPs have been used in high-throughput screens (HTS) to identify small molecules that target  $\text{IMP}\alpha/\beta$ -dependent nuclear import of viral proteins central to infection for Human Immunodeficiency Virus, dengue, and Venezuelan Equine Encephalitis Virus [19–24]. Importantly, a number of these, including ivermectin, which is of current interest with respect to SARS-CoV-2, have been shown to limit viral infection by preventing the host  $\text{IMP}\alpha$  recognition/nuclear localization of viral proteins in infected cells [19,20,22–30]. Clearly, inhibitors of nuclear transport machinery have considerable therapeutic potential [17–20,26,31].

The fact that *P. falciparum* and *T. gondii* divide rapidly within the human host implies a need for efficient nuclear transport systems [32], raising the possibility that the nuclear trafficking pathways of apicomplexans could serve as targets for therapeutics to limit infection. Importantly, in this context, both *P. falciparum* and *T. gondii* have a single genomic copy of  $\text{IMP}\alpha$  [9] that is essential [33,34]. *P. falciparum*  $\text{IMP}\alpha$  (PfIMP $\alpha$ ) is known to bind to a “classical NLS” identified in *P. falciparum* trimethyl guanosine synthase 1 (TGS1) that methylates the terminal phosphate groups of spliceosomal RNAs [35,36], yet appears to show a unique lack of autoinhibition [37], which as indicated above, is central to the function of mammalian  $\text{IMP}\alpha$ s [15,16]. Apicomplexan  $\text{IMP}\alpha$  would appear to be an intriguing prospect as a target for inhibitors to limit diseases caused by *P. falciparum* and *T. gondii*.

Here we describe, for the first time, a high-throughput screen (HTS) to identify small molecule inhibitors of PfIMP $\alpha$ : TGS1-NLS interaction using AlphaScreen technology [21–23,38]. In total, 13 small molecules of interest were identified as hits and screened for their ability to inhibit interaction between mammalian  $\text{IMP}\alpha$  and *T. gondii*  $\text{IMP}\alpha$  (TgIMP $\alpha$ ) and the well-characterized Simian Virus 40 T-antigen (SV40 T-ag) NLS, with the compound Bay 11-7085 showing high selectivity for PfIMP $\alpha$ . Thermostability assays were used to confirm the direct binding of Bay 11-7085 and other compounds to PfIMP $\alpha$ , and their ability to inhibit growth by both *P. falciparum* and *T. gondii* was also confirmed. The results establish the principle that apicomplexan  $\text{IMP}\alpha$  is a viable target for drug discovery to combat malaria as well as toxoplasmosis.

## 2. Materials and Methods

### 2.1. Plasmid Construction

All restriction enzymes were obtained from Thermo Fisher Scientific (Waltham, MA, USA), and gene amplification was performed using the KAPA HiFiTM PCR kit (Kapa Biosystems, Wilmington, MA, USA) unless otherwise indicated. Primers were procured from Integrated DNA Technologies (IDT, Coralville, IA, USA). The integrity of all plasmid constructs was confirmed by DNA sequencing.

To generate a TgIMP $\alpha$  C-terminal His-tagged bacterial expression construct, the TgIMP $\alpha$  coding sequence was PCR-amplified from cDNA and inserted between the NcoI and HindIII restriction sites of plasmid vector pET28a. Primers used to amplify the TgIMP $\alpha$  gene were (Forward: 5' CATGCCATGGAGCGCAAGTTGGCCGATC 3', Reverse: 5' TCCCAAGCTTCTGGCCGAAGTTGAAGCCTC 3'; restriction sites underlined).

To generate a C-terminal glutathione S-transferase (GST) fusion protein expression construct in plasmid vector pET28a in place of the C-terminal hexa-Histidine tag, the

GST coding sequence was PCR amplified from plasmid pGEX-6p1 and inserted into the NheI and HindIII restriction sites of pET28a. The primers used to amplify the GST gene sequence were (Forward: 5' CTAGCTAGCTCCCTATACTAGGTTATTGG 3' and Reverse: 5' CCCAAGCTTTCAGTCACGATGCG 3'; restriction sites underlined). *P. falciparum* (PlasmoDB ID: PF3D7\_0812400) and *T. gondii* IMP $\alpha$  (ToxoDB ID: TGGT1\_252290) with C-terminal hexa-Histidine tags were subcloned as PCR products into the NcoI and NheI sites of the pET28a-C GST vector. The primers used for PCR amplification were as follows: (PfIMP $\alpha$ : Forward: 5' CATGCCATGGATAGGAGAATAGAAGCTAG 3'; Reverse: 5' CTAGCTAGCGTCAAATGTAAAAT-CCCTATTATAAAC 3'; TgIMP $\alpha$ : Forward: 5' CATGCCATGGAGCGCAAGTTGGCCG 3'; Reverse: 5' CTAGCTAGCCTGGCCGAAGT TGAAGCC 3'; restriction sites underlined), with PfIMP $\alpha$  amplified from the previously described hexa-Histidine-tagged expression construction [37], and TgIMP $\alpha$  amplified from a construct generated in identical fashion.

## 2.2. Protein Expression, Purification, and Use in AlphaScreen Assay

PfIMP $\alpha$ , TgIMP $\alpha$ , *Mus musculus* IMP $\alpha$  (MmIMP $\alpha$ ),  $\Delta$ IBBMmIMP $\alpha$ , and  $\beta$ 1 (MmIMP $\beta$ ) GST fusion proteins were expressed and purified essentially as previously [21–23]. His-tagged TGS1-NLS-GFP, PfIMP $\alpha$  and TgIMP $\alpha$  proteins were purified using Ni<sup>2+</sup>-affinity chromatography as described [37]. His-tagged SV40 T-ag-NLS-GFP was purified as previously [38]. Biotinylation of GST-tagged proteins was carried out using the Sulfo-NHS-Biotin reagent (Pierce, Rockford, IL, USA) as described previously [21]. AlphaScreen binding assay was performed as described previously [21–24,27–30,38].

## 2.3. HTS

HTS in the AlphaScreen system was performed robotically as previously [21–23] to identify inhibitors of PfIMP $\alpha$ : TGS1 NLS-GFP interaction from the MMV Pathogen Box Chemical Library (400 compounds; Medicines for Malaria Venture, Geneva, Switzerland) and Library of Pharmacologically Active Compounds (LOPAC1280; Sigma-Aldrich, St Louis, MO, USA; 1280 compounds). Then, 10 nM biotinylated PfIMP $\alpha$  and 60 nM TGS1-NLS-GFP were used with library compounds, screened at 10  $\mu$ M final concentration.

Briefly, 5  $\mu$ L of each compound in DMSO was added to quadruplicate wells of a 384-well plate along with appropriate controls including DMSO alone and ivermectin, as previously [23], using a JANUS Modular Dispense Technology (MDT) robotic system (PerkinElmer, Waltham, MA, USA). This was followed by successive 7 and 5  $\mu$ L additions, respectively, of PfIMP $\alpha$  (10 nM) and TGS1-NLS-GFP (60 nM) or PBS (“no bait” control), respectively, and 30 min incubation at room temperature. AlphaScreen acceptor beads (1/40 dilution of Ni-NTA beads and 6.25 % BSA in PBS) were then added to each well using a Multidrop liquid dispenser (Thermo Fisher Scientific, Waltham, MA, USA) and the plates incubated for 90 min at room temperature in the dark. Then, 4  $\mu$ L of the AlphaScreen donor beads (1/40 dilution of GSH. acceptor beads in PBS) was finally added to each well using a Multidrop, followed by a further incubation of 2 h at room temperature in the dark.

Plates were read for an Alphascreen signal on an Envision plate reader (PerkinElmer, Waltham, MA, USA), with signals from the negative control wells (no bait control) on each plate subtracted. Compounds showing more than 70% inhibition (DMSO negative control = 100%) were tested to exclude false-positives by counter-screening in the system using 5 nM hexa-His-Biotin in place of hexa-His-tagged and biotinylated proteins [21–23].

## 2.4. Thermostability Assay (TSA)

The effect of inhibitory compounds on IMP $\alpha$  thermostability was tested, as previously, using the fluorescent dye SYPRO Orange (Thermo Fisher Scientific, Waltham, MA, USA) and the Qiagen Rotor-Gene Q6 plex instrument programmed in the melt curve mode [28,30]. Increasing concentrations of compound in 0.5  $\mu$ L DMSO were added to 24.5  $\mu$ L recombinant protein (2  $\mu$ M) in phosphate-buffered saline (PBS). Next, 1  $\mu$ L of SYPRO Orange dye was added, the reaction mixture heated at 0.5  $^{\circ}$ C/min from 27  $^{\circ}$ C to 90  $^{\circ}$ C, and the

fluorescence intensity caused by the SYPRO Orange binding to the proteins monitored (excitation/emission: 530/555 nm).  $T_m$  is the temperature at which 50% of the protein is unfolded.

### 2.5. *P. falciparum* Culture and Growth Inhibition Assay

Red blood cells (RBCs) were derived from blood from volunteers (approval from the Institute Ethics Committee, IIT Bombay, Mumbai, India) by density gradient centrifugation. Aliquots of cryopreserved *P. falciparum* 3D7 strain in human red blood cells (RBCs—3% hematocrit, <5% parasitemia) were thawed and cultured using RPMI (Roswell Park Memorial Institute) 1640 medium supplemented with 0.5% Albumax (Gibco™, Waltham, MA, USA), 50 mg/L hypoxanthine (Sigma-Aldrich, St Louis, MO, USA), 2 g/L D-glucose (Sigma-Aldrich, St Louis, MO, USA), 2 g/L sodium bicarbonate (Sigma-Aldrich, St Louis, MO, USA), and 56 mg/L of gentamicin (Abbott, Chicago, IL, USA) at 37 °C in 5% CO<sub>2</sub> in a humidified incubator according to the standard procedures [39]; suspension cultures were maintained at 3% hematocrit and <5% parasitemia, by adding a fresh medium daily and a regular addition of fresh human RBCs.

Before growth inhibition assays, cultures were synchronized using 5% D-sorbitol (Sigma-Aldrich, St Louis, MO, USA) predominantly to obtain the ring stage of the *P. falciparum* life cycle. The test compounds auranofin, Bay 11-7085, CAPE (all from Sigma-Aldrich, St Louis, MO, USA) and Zoxazolamine-MMV003270 (MMV, Geneva, Switzerland) were made up at a stock concentration of 10 mM in DMSO and diluted in RPMI as required for growth inhibition studies or IC<sub>50</sub> analysis, with dihydroartemisinin (gift from IPCA Laboratories, Mumbai, India) used as a control.

Growth assays in the absence and presence of inhibitors were performed using the Histidine-Rich Protein 2 (HRP2) sandwich horseradish peroxidase-linked immunosorbent assay to measure HRP2 protein levels as an indicator of growth [40,41]. Briefly, 25 µL of compound was added to 96-well microculture plates (Eppendorf, Hamburg, Germany) of 0.25% (with fresh RBCs), and added at a hematocrit of 3%. The plates were then incubated for 72 h at 37 °C in a humidified incubator, sparged with 5% CO<sub>2</sub>. 72 h later, the plates were subjected to freeze–thaw to achieve hemolysis, and samples diluted 200-fold in H<sub>2</sub>O in transferring to another plate. A day prior to analysis, 96-well ELISA plates (Sigma-Aldrich, St Louis, MO, USA) were coated overnight at 4 °C with 100 µL of 1 µg/mL IgM capture antibody MPFM-55A (Immunology Consultants Laboratory, Portland, OR, USA) specific for *P. falciparum* HRP2. After blocking for 2 h at room temperature with 2% BSA in PBS, diluted samples were added to the wells, followed by incubation for 2 h, then the plates were washed three times with 0.05% Tween 20 in PBS. Next, 100 µL of the secondary antibody MPFG-55P (Immunology Consultants Laboratory, Portland, OR, USA) conjugated with horseradish peroxidase (0.25 µg/mL in PBS with 2% BSA) was then added to each well, and the plates incubated for 1 h at room temperature, prior to being washed three times, and 100 µL 3,3', 5,5' tetramethylbenzidine substrate (BD Biosciences, San Jose, CA, USA) being added. After 10 min incubation in the dark, 50 µL of 1 M H<sub>2</sub>SO<sub>4</sub> was added and the absorbance was read at 450 nm on a Multiscan™ FC Microplate Spectrophotometer (Thermo Fisher Scientific, Waltham, MA, USA).

### 2.6. *T. gondii* Tachyzoite Culture and Growth Inhibition Assay

*T. gondii* RH strain expressing the luciferase reporter (RH-Fluc) was derived to assess the effect of the inhibitors on growth. Briefly, plasmid pCTG-EGFP [42] was modified by replacing the coding sequence of EGFP with that of the firefly luciferase reporter, using restriction enzymes BglII and PstI (Thermo Fisher Scientific, Waltham, MA, USA). The resultant plasmid, pCTG-Fluc, expressing firefly luciferase constitutively under the control of the *T. gondii* TubulinA promoter, was electroporated into the *T. gondii* RH strain [43,44] using a Bio-Rad GenePulser Xcell system (1500 V, 50 Ω and 25 µF) along with restriction enzyme NotI to initiate RE-Mediated Integration (REMI) of the linearized plasmid into the genome [45,46]. The resultant stable *T. gondii* line expressing the luciferase reporter

was selected for resistance to 20  $\mu$ M chloramphenicol (encoded by the plasmid pCTG), and dilution cloning [47] was performed to ultimately identify the clone (RH-Fluc) with the highest luciferase activity (c.  $4 \times 10^7$  RLU from  $10^7$  parasites) used for growth assays. *T. gondii* tachyzoites were maintained and cultured at 37 °C in 5% CO<sub>2</sub> in a humidified incubator in primary human foreskin fibroblasts (HFF, ATCC) [47,48]; HFF cells were maintained in Dulbecco's modified Eagle medium (DMEM) (Gibco™, Waltham, MA, USA) supplemented with 3.7 g/L sodium bicarbonate and 2.38 g/L HEPES, 10% Cosmic Calf serum (Hyclone™, Logan, UT, USA) and 20 mg/L gentamicin [47,48].

Growth inhibition was assessed by luminescence measurements as described [49,50]. Briefly, 100  $\mu$ L of culture medium with or without inhibitors was added to confluent monolayers of HFF cells grown in 96-well treated culture plates (Eppendorf, Hamburg, Germany), followed by 100  $\mu$ L of DMEM containing 5000 parasites. After 48 h, 150  $\mu$ L of the culture media was discarded from each well without aspirating any parasites, and 10  $\mu$ L lysis buffer was added to lyse the parasites, followed by 50  $\mu$ L of 2 $\times$  luciferase assay reagent (Promega, Madison, WI, USA). Luminescence was measured directly for 10 s using a Varioskan™ LUX multimode microplate reader (Thermo Fisher Scientific, Waltham, MA, USA).

### 2.7. MTT Assay for Host Cell Cytotoxicity

The MTT assay was used to measure the cytotoxicity of the small molecules against the HFF cells as described [51]. Briefly, freshly confluent HFF cells in a 96-well culture plate were treated with increasing concentrations of compounds for 48 h, prior to the MTT assay.

### 2.8. Statistical Analysis

Four parameter dose response curves were fitted using non-linear regression analysis in GraphPad Prism 9.2.0 (San Diego, CA, USA) using the formula:  $y = a + ((b - a) / (1 + 10^{-(\log(c) - x) \times d}))$ , where  $a$  is the minimum asymptote,  $b$  is the maximum asymptote,  $c$  is the half-maximal inhibitory concentration value (IC<sub>50</sub>) and  $d$  is the slope at the steepest part of the curve (the Hill slope).

## 3. Results

### 3.1. Optimisation of AlphaScreen Binding Assay for HTS

HTS was performed using a roboticised AlphaScreen system, as previously [21–23], to identify small molecules inhibiting the interaction of PfIMP $\alpha$  and the *P. falciparum* TGS1 NLS [37]. Unlike mammalian IMP $\alpha$ , full-length PfIMP $\alpha$  lacks autoinhibition, not requiring IMP $\beta$ 1 for high affinity binding to NLSs [37]. This is illustrated in Figure 1, where NLS-binding by full-length PfIMP $\alpha$  is compared to that for Mm $\Delta$ IBBIMP $\alpha$ , a form of *M. musculus* IMP $\alpha$  deleted for the autoinhibitory IBB domain. PfIMP $\alpha$  shows high-affinity binding (dissociation constant,  $K_d$ , of 6.5 nM) to the TGS1 NLS, comparable to that for Mm $\Delta$ IBBIMP $\alpha$  binding to the well-characterized simian virus SV40 large tumor antigen (T-ag) (Figure 1; see legend). Based on these results and further optimization in the robotic system (not shown), the concentrations of PfIMP $\alpha$  and TGS1-NLS-GFP selected for use in HTS were fixed to 10 and 60 nM, respectively, giving c. 70% maximal AlphaScreen signal, with the possibility to identify agents either inhibiting or enhancing the signal [21–23].

### 3.2. Library Screening for Inhibitors of the Interaction between PfIMP $\alpha$ and TGS1-NLS

Using the assay optimized in Section 3.1, HTS was performed essentially, as previously [23], to identify inhibitors of the interaction between PfIMP $\alpha$  and the TGS1-NLS (see Figure 2A), using the LOPAC and Pathogen Box chemical libraries; compounds were screened in quadruplicate, together with appropriate controls as previously [23]. The assay's robustness was confirmed by the Z' factor (values > 0.5 across all plates, with a median of 0.75—see Figure 2B) [52]. Compounds inhibiting the maximum signal compared to the DMSO control by >70% were counter-screened as previously for interference with the AlphaScreen assay, where biotinylated and His-tagged proteins were replaced

with biotinylated-His, which generated a strong AlphaScreen signal [21–23]. Ultimately, 13 compounds were selected for further analysis, as outlined in Figure 2A (see below). These included auranofin/MMV688978, which was identified as a strong hit from both the LOPAC and Pathogen Box libraries.

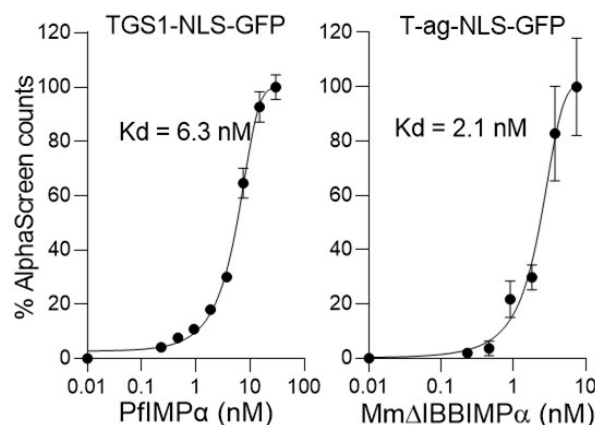


**Figure 1.** PfIMPα shows high affinity binding to the TGS1 NLS, comparable to that for MmΔIBBIMPα. AlphaScreen technology was used to determine the  $K_d$  value of NLS-GFP (30 nM) binding to biotinylated-GST-IMPαs (5 nM). Data points in the figures represent the AlphaScreen signal for NLS-GFP and IMPα interaction from a single typical experiment from a series of three independent experiments. Pooled data showed  $K_d$  values of  $6.5 \pm 0.2$  and  $2.6 \pm 0.5$  nM (mean  $\pm$  SEM,  $n = 3$ ) for PfIMPα:TGS1-NLS and MmΔIBBIMPα:T-ag-NLS, respectively.

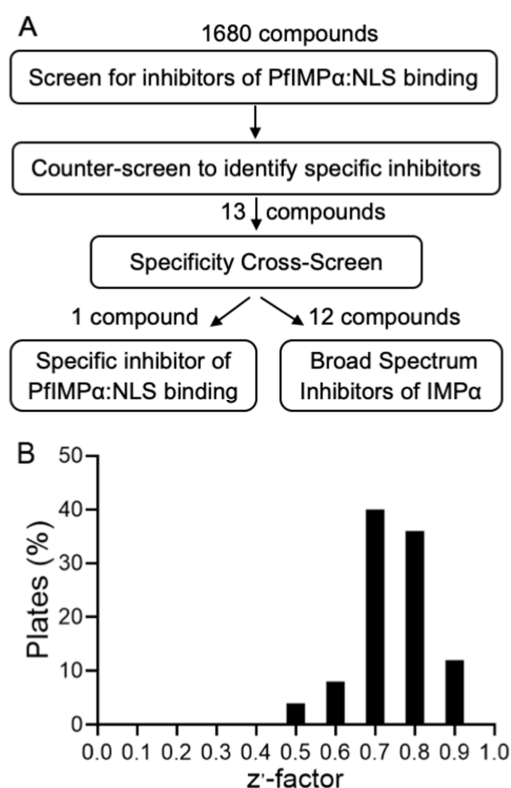


**Figure 2.** HTS to identify inhibitors of PfIMPα:NLS binding. (A) Schematic showing the strategy used to identify inhibitors of PfIMPα:NLS binding in the AlphaScreen system from the LOPAC and Pathogen Box libraries; the numbers of compounds at different stages of the screening/counter-screening process are indicated. (B) Plot of distribution of  $Z'$  factors for the HTS, calculated as previously [21–23,52], as a % of the number of plates.

### 3.3. Cross-Screening to Identify Selective Inhibitors of PfIMP $\alpha$ :TGS1-NLS Binding

To determine the extent to which the hit compounds may be selective for PfIMP $\alpha$ , we compared their ability to inhibit NLS binding by PfIMP $\alpha$ , mammalian non-autoinhibited MmIMP $\alpha$  (Mm $\Delta$ IBBIMP $\alpha$ ) as well as the MmIMP $\alpha$ / $\beta$  heterodimer, and the apicomplexan *T. gondii* IMP $\alpha$  (TgIMP $\alpha$ ). The results are summarized in Table 1; all compounds inhibit PfIMP $\alpha$  by 70% or more, with a cut-off of 50% inhibition or higher used to assess selectivity. “General inhibitors” thus block interactions between all of the four IMP-NLS interactions by at least 50%, whereas “selective inhibitors” inhibit a subset of the IMP-NLS interactions by 50% or more.

**Table 1.** Selectivity of PfIMP $\alpha$  inhibitors.

Hit Compound <sup>x</sup>	% Inhibition of IMP $\alpha$ -NLS Interaction <sup>*</sup>			
	PfIMP $\alpha$	TgIMP $\alpha$ <sup>#</sup>	Mm $\Delta$ IBBIMP $\alpha$	MmIMP $\alpha$ / $\beta$
<b>(A) General Inhibitors</b>				
MMV688978 (auranofin)	94	90	91	100
Daphnetin	81	70	81	83
Chelerythrine Cl	81	67	88	94
AC-93253 iodide	82	72	67	62
MMV003270	92	83	82	NT <sup>§</sup>
6-Fluoronorepinephrine HCl	77	67	60	51
<b>(B) Inhibitors Showing Selectivity</b>				
<b>(B1) Selective for PfIMP<math>\alpha</math></b>				
Bay 11-7085	75	0	9	14
<b>(B2) Selective for IMP<math>\alpha</math>s</b>				
Caffeic acid phenethyl ester	84	62	92	14
<b>(B3) Others</b>				
MMV030734	99	44	43	68
MMV024937	73	26	70	24
(–)-Epinephrine bitartrate	85	23	34	94
(±)-Epinephrine HCl	98	24	35	95
MMV676512	100	48	54	100

<sup>\*</sup> Results represent the average percentage (%) inhibition of the AlphaScreen signal relative to the 1% DMSO control tested in quadruplicate, with compounds at 10  $\mu$ M and protein concentrations as follows: PfIMP $\alpha$  (10 nM):TGS1-NLS-GFP (60 nM),  $\Delta$ IBBMmIMP $\alpha$  (5 nM):T-ag-NLS-GFP (30 nM), MmIMP $\alpha$ / $\beta$  (5 nM):T-ag-NLS-GFP (30 nM) and TgIMP $\alpha$  (5 nM):T-ag-NLS-GFP (30 nM). <sup>x</sup> All compounds inhibit PfIMP $\alpha$ :NLS > 70%; a cut-off of 50% inhibition is arbitrarily used for the working categories in A and B (highlighted by blocking). <sup>#</sup>  $K_d$  for TgIMP $\alpha$  (5 nM):T-ag-NLS-GFP (30 nM) binding without inhibitors is  $3.5 \pm 1$  nM ( $n = 3$ ). <sup>§</sup> NT, not tested.

At 10  $\mu$ M, 11 of the compounds showed stronger inhibition of the PfIMP $\alpha$ :NLS interaction than of the Mm $\Delta$ IBBIMP $\alpha$ :NLS or TgIMP $\alpha$ :NLS interactions (Table 1), indicating overall selectivity towards PfIMP $\alpha$ . Daphnetin was an exception in that it inhibited PfIMP $\alpha$  and Mm $\Delta$ IBBIMP $\alpha$  to the same extent, whilst caffeic acid phenethyl ester (CAPE) showed higher inhibition of Mm $\Delta$ IBBIMP $\alpha$  than PfIMP $\alpha$  (Table 1). A number of compounds (Table 1A) showed >50% inhibition of all four IMP-NLS binding interactions, with the implication that they are “general” inhibitors of IMP $\alpha$ , even in the context of the IMP $\alpha$ / $\beta$  heterodimer. The other inhibitors showed various degrees of selectivity, inhibiting one or a subset of the IMP-NLS interactions, although not all.

Bay 11-7085 appeared to be highly selective for PfIMP $\alpha$  (75% inhibition) with 0–14% inhibition of the other IMP $\alpha$ s and the MmIMP $\alpha$ / $\beta$  heterodimer (Table 1). MMV030734 showed a similar trend, however showed 68% inhibition of MmIMP $\alpha$ / $\beta$ ; interestingly, MMV030734, MMV676512 and (±)-epinephrine HCl were the most potent inhibitors of PfIMP $\alpha$  ( $\geq 98\%$  inhibition), all inhibited TgIMP $\alpha$  and Mm $\Delta$ IBBIMP $\alpha$  to <55%, and all inhibited MmIMP $\alpha$ / $\beta$  (in the case of MMV676512 and (±)-epinephrine HCl to  $\geq 95\%$ ). Finally, based on the 50% inhibition criterion, CAPE was the only inhibitor that inhibited all three IMP $\alpha$ s, yet did not inhibit MmIMP $\alpha$ / $\beta$  (Table 1).

Based on the cross-screen analysis, auranofin, Bay 11-7085, CAPE, MMV003270 were subjected to  $IC_{50}$  analysis for the three IMP $\alpha$ :NLS interactions (see Table 2), and the results generally indicated low  $\mu$ M values and support the conclusions from Table 1 with respect to selectivity. The results for Bay 11-7085, for example, indicate c. 16 and 12-fold higher  $IC_{50}$  values for inhibition of the TgIMP $\alpha$ -NLS and  $\Delta$ IBBMmIMP $\alpha$ -NLS interactions, respectively, (31 and 23  $\mu$ M values) compared to that for the PfIMP $\alpha$ -TGS-NLS interaction (2  $\mu$ M) (Figure 3, Table 3), supporting the idea that Bay 11-7085 is highly selective for PfIMP $\alpha$ . Auranofin, in contrast, showed robust inhibition ( $IC_{50}$  values of 60–80 nM) of all three IMP $\alpha$ :NLS interactions (Figure 3), consistent with it being a strong general inhibitor; CAPE ( $IC_{50}$  values of 0.7–2.9  $\mu$ M) and MMV003270 ( $IC_{50}$  values of 200–400 nM) showed a similar inhibitory profile, although they were not as potent (see Table 3).

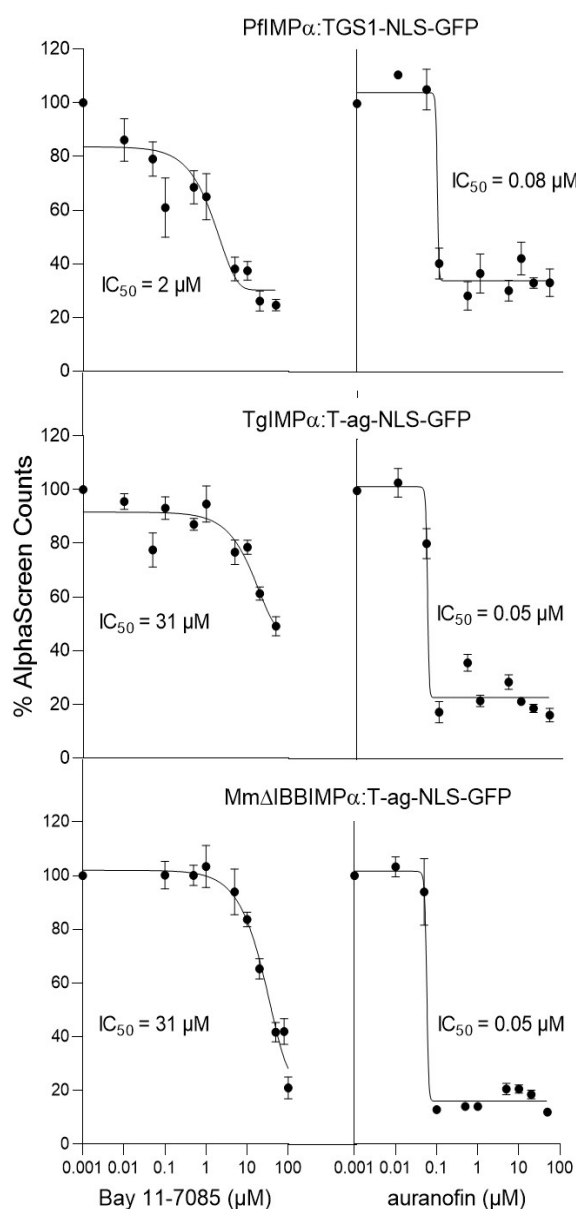


**Figure 3.** Bay 11-7085 specifically inhibits PfIMP $\alpha$ -TGS1-NLS interaction at low micromolar concentration, whereas auranofin is a general inhibitor of IMP $\alpha$ :NLS interactions. AlphaScreen technology was used to determine the  $IC_{50}$  for inhibition by Bay 11-7085 and auranofin binding of IMP $\alpha$ s (5 nM) to NLS (30 nM). Data represent the mean  $\pm$  SEM ( $n = 4$ ) from a single experiment, from a series of three independent experiments (see Table 3 for pooled data).

**Table 2.** Summary of the IC<sub>50</sub> values for inhibition of IMP $\alpha$ :NLS interactions.

Binding Interaction	IC <sub>50</sub> ( $\mu$ M) *			
	Bay 11-7085	CAPE	Auranofin	MMV003270
PfIMP $\alpha$ :TGS1-NLS-GFP	1.9 $\pm$ 0.1	1.8 $\pm$ 0.3	0.07 $\pm$ 0.01	0.3 $\pm$ 0.2
TgIMP $\alpha$ :T-ag-NLS-GFP	30.4 $\pm$ 0.6	2.9 $\pm$ 0.9	0.08 $\pm$ 0.01	0.2 $\pm$ 0.1
Mm $\Delta$ IBBIMP $\alpha$ :T-ag-NLS	23.4 $\pm$ 2.9	0.7 $\pm$ 0.1	0.06 $\pm$ 0.01	0.4 $\pm$ 0.2

\* Results represent the mean  $\pm$  SEM ( $n = 3$ ) for IC<sub>50</sub> values measured as per Figure 3.

### 3.4. Bay 11-7085 and Auranofin Appear to Bind Directly to IMP $\alpha$

A thermostability assay (TSA) was used as previously [28,30] to examine direct binding of the compounds to the different IMP $\alpha$ s. PfIMP $\alpha$ , TgIMP $\alpha$  and MmIMP $\alpha$  were all similar in showing stability up to c. 43–45 °C in the absence of the inhibitor compounds (see also [28,30]). Although MMV003270 could not be sourced in sufficient amounts for the assay, we tested the PfIMP $\alpha$  selective inhibitor Bay 11-7085, the general inhibitor auranofin, and the IMP $\alpha$  selective inhibitor CAPE. The latter did not elicit any marked change in stability for any of the IMP $\alpha$ s up to 100  $\mu$ M, with the possible exception being for PfIMP $\alpha$ , where concentrations of 75  $\mu$ M or higher elicited a slight increase of 2 °C in thermostability (to 47 °C—see Figure 4 left panel); both Bay 11-7085 and auranofin, in contrast, had marked effects on thermostability of all three IMP $\alpha$ s, consistent with the idea that they bind directly to the IMP $\alpha$ s, thereby altering IMP $\alpha$  structure and thereby thermostability. Auranofin at concentrations as low as 5  $\mu$ M appeared to reduce thermostability in the case of all three IMP $\alpha$ s (stable only up to 32–35 °C) by 12–15 °C (Figure 4). Bay 11-7085 at 10–20  $\mu$ M similarly reduced the thermostability (9–15 °C) of both TgIMP $\alpha$  and MmIMP $\alpha$  (stable only up to 30–36 °C—Figure 4 middle and right panels). Strikingly, however, it appeared to have a biphasic effect on PfIMP $\alpha$ , concentrations up to 10  $\mu$ M reducing stability by 6 °C (to 39 °C), and concentrations higher than 20  $\mu$ M increasing stability by 9–11 °C (to 48–50 °C—Figure 4 left panel). Whether these effects could indicate the more than one binding mode/site for Bay 11-7085 on PfIMP $\alpha$  will require detailed experimental investigation in the future, however, the clear implication is that Bay 11-7085 binds to PfIMP $\alpha$  in a mode quite distinct to that of auranofin, and quite distinct to the effect of its binding on the other IMP $\alpha$ s; this may well be the basis of the observations from the binding assays (Figure 3, Table 2) that show that although they are able to inhibit NLS binding by both MmIMP $\alpha$  and TgIMP $\alpha$ , they do so only at concentrations 12–16 times higher than those required to inhibit NLS binding by PfIMP $\alpha$ .

### 3.5. PfIMP $\alpha$ Inhibitors Limit Proliferation of *P. falciparum* and *T. gondii* In Vitro

To begin to assess formally the importance of NLS recognition by *P. falciparum* and *T. gondii* IMP $\alpha$  in a physiological context, we screened the compounds against both parasites at a single concentration (10  $\mu$ M). For *P. falciparum*, we employed the standard HRP2-based (histidine-rich protein 2) ELISA, with the clinically prescribed drug dihydroartemisinin (DHA) as a positive control against *P. falciparum* at 10  $\mu$ M [40,41,53]. Initial analysis showed that auranofin and CAPE showed >50% inhibition at 10  $\mu$ M (Figure 5A); Bay 11-7085 showed c. 20% inhibition. The basis for Bay 11-7085's relatively low activity in this assay is unclear, however, it may relate to the limited ability of the compound to be taken up by the malarial parasite, or low stability (see Section 4).

For *T. gondii*, we used tachyzoites constitutively expressing luciferase (see Section 2.6), with the clinically prescribed toxoplasmosis drug pyrimethamine used as a positive control [54]. A > 50% reduction in luciferase activity, indicative of growth inhibition, was effected at 10  $\mu$ M by auranofin and Bay 11-7085, however, CAPE showed only 5% inhibition (Figure 5B). As for Bay 11-7085 above, the basis for the low activity in this assay is unclear although it may relate to the poor uptake of the compound by the tachyzoites, or reduced stability (see Section 4); interference with the luciferase chemistry seems unlikely (e.g., see [55]).

Detailed IC<sub>50</sub> analysis for activity against *P. falciparum* was performed for auranofin and CAPE, with results indicating values in the low  $\mu\text{M}$  range (Figure 6, Table 3 central column); clearly, both have robust antimalarial activity. In parallel, detailed IC<sub>50</sub> analysis were similarly carried out for Bay 11-7085 and auranofin with respect to *T. gondii*; results indicated robust antiparasitic activity, with IC<sub>50</sub> values in the low  $\mu\text{M}$  concentration range (Figure 7; Table 3 right column).

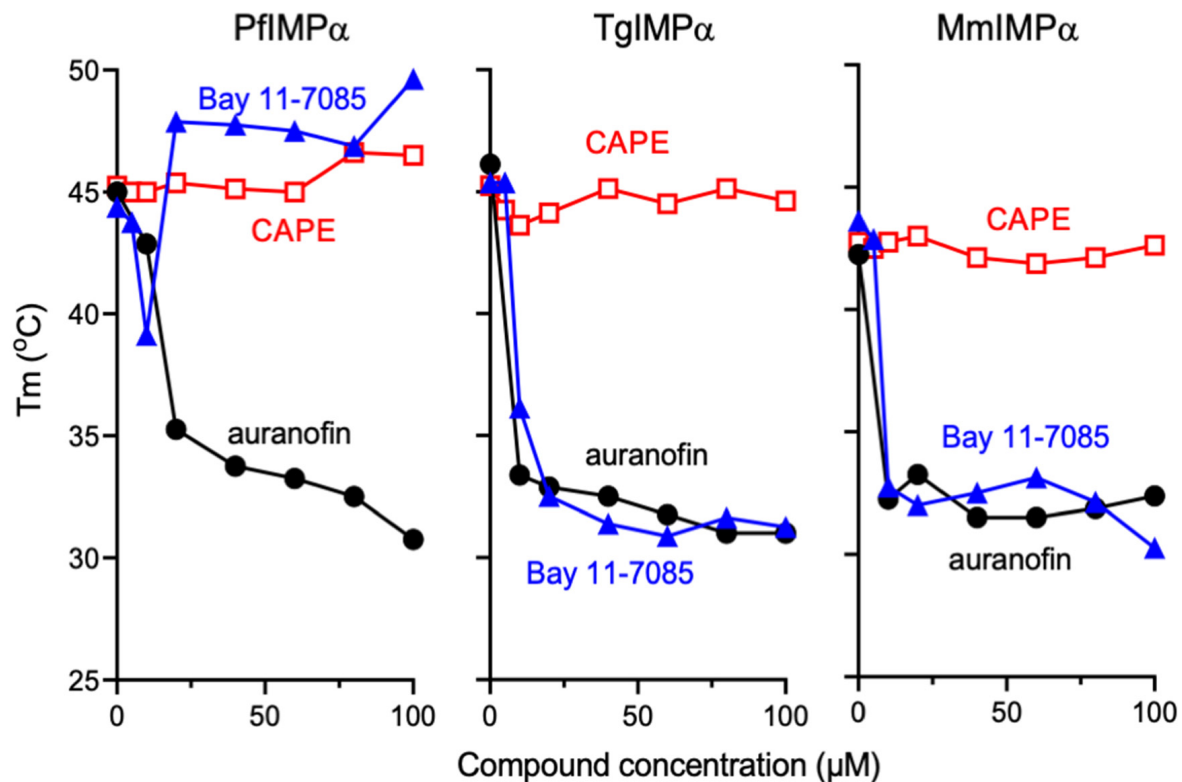


**Figure 4.** Bay 11-7085 and auranofin appear to bind directly to IMP $\alpha$ s as indicated by thermostability analysis. The indicated His6-tagged IMP $\alpha$  proteins were subjected to thermostability analysis in the presence of increasing concentrations in the indicated compounds. Results are from a single experiment, representative of three independent experiments.

**Table 3.** Summary of the IC<sub>50</sub> values for inhibition of *P. falciparum* and *T. gondii* parasites by IMP $\alpha$  inhibitors in culture.

Compound	IC <sub>50</sub> ( $\mu\text{M}$ ) *	
	<i>P. falciparum</i>	<i>T. gondii</i>
auranofin	1.9 $\pm$ 0.5	2.3 $\pm$ 0.8
CAPE	7.5 $\pm$ 1.1	>10 #
Bay 11-7085	>10 #	2.7 $\pm$ 0.7
DHA	0.001 $\pm$ 0.0005	NT <sup>x</sup>
pyrimethamine	NT <sup>x</sup>	0.46 $\pm$ 0.14 ^

\* Results represent the mean  $\pm$  SD ( $n = 3$ ) for IC<sub>50</sub> values determined as per Figures 6 and 7. # See Figure 5. <sup>x</sup> NT, not tested. ^ See also [54].

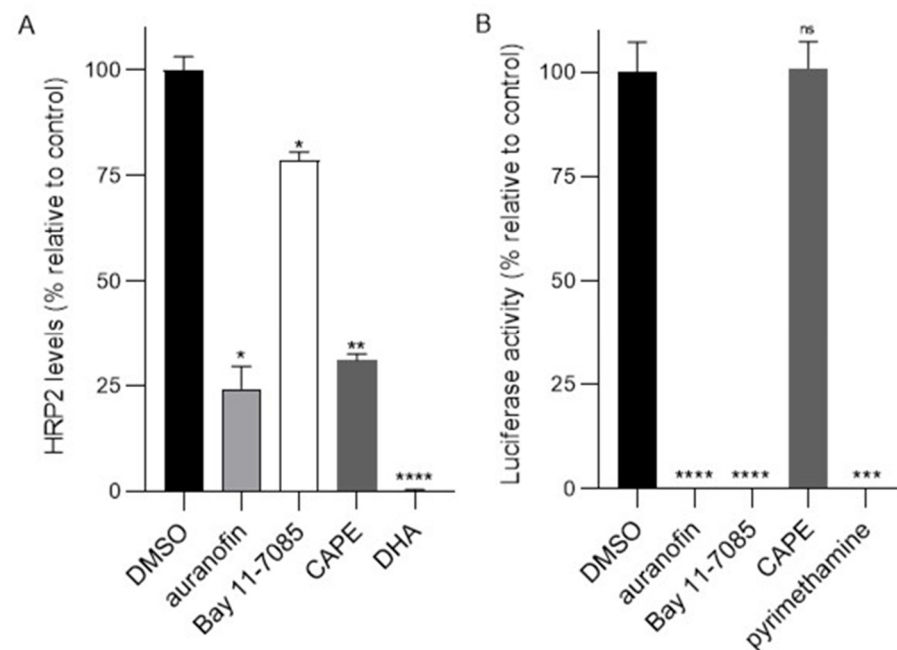


**Figure 5.** Results for the initial screening of selected hit compounds for antimalarial activity towards *P. falciparum* (A) and *T. gondii* (B). (A) *P. falciparum* cultures (0.25% parasitemia) were treated with 10  $\mu$ M concentration of the indicated compounds for 72 h, after which the HRP2-based sandwich ELISA was used to measure the HRP2 levels determined by optical density. Results are from a single typical experiment performed in duplicate (SD shown), representative of a series of three independent experiments. \*,  $p < 0.05$ ; \*\*,  $p < 0.01$ ; \*\*\*,  $p < 0.0001$ . (B) HFF cells infected with RH-Fluc *T. gondii* parasites were incubated with 10  $\mu$ M c of the indicated compounds for 48 h, after which parasite growth was measured using a luciferase assay. Results are from a single typical experiment performed in duplicate (SD shown), representative of a series of three independent experiments. \*\*\*,  $p < 0.001$ ; \*\*\*\*,  $p < 0.0001$ ; ns, not significant.

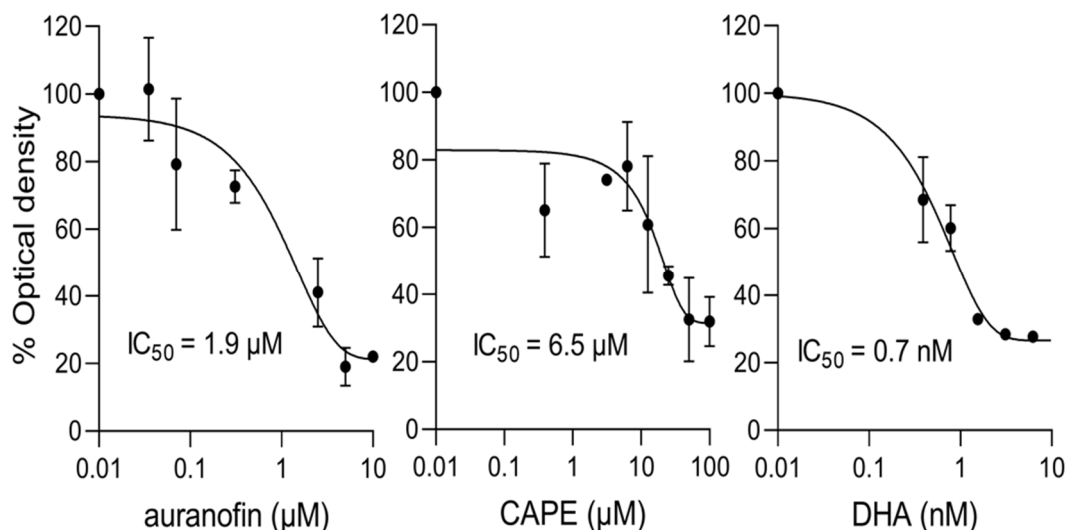


**Figure 6.** Auranofin and CAPE inhibit *P. falciparum* parasites grown in culture at low  $\mu$ M concentrations. *P. falciparum* cultures (0.25% parasitemia) were treated with increasing concentrations of the indicated compounds for 72 h, after which the HRP2-based sandwich ELISA was used to measure the HRP2 levels, determined by optical density. Results shown are from a single typical experiment performed in duplicate (SD shown), representative of a series of three independent experiments (see Table 3 for pooled data).

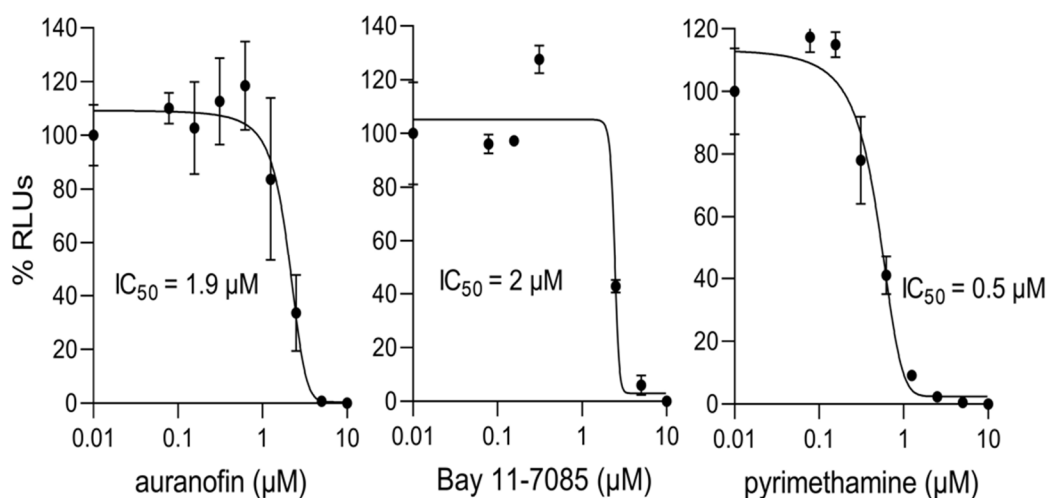


**Figure 7.** Auranofin and Bay 11-7085 inhibit *T. gondii* in vitro at low  $\mu\text{M}$  concentrations. HFF cells infected with RH-Fluc parasites were incubated with increasing concentrations of the indicated compounds for 48 h. Parasite growth was measured using a luciferase assay. Results shown above are from a single typical experiment performed in duplicate (SD indicated), from a series of three independent experiments (see Table 3, right column, for pooled data).

To confirm that the above effects were not attributable to cytotoxicity effected by the compounds on the HFF cells used in the *T. gondii* infectious system, HFF cells were treated with Bay 11-7085 and auranofin and viability monitored using the MTT assay, as previously. Auranofin and Bay 11-7085 showed  $\text{CC}_{50}$  values for HFF cells of five and eight  $\mu\text{M}$ , respectively, (Figure S1, Table S1), corresponding to selectivity index values of two (auranofin) and three (Bay 11-7085) (Table S1). What is clear is that at concentrations  $< 5 \mu\text{M}$ , cytotoxicity is essentially absent; since parasite killing at 2  $\mu\text{M}$  or less is substantial ( $\geq 60\%$ —see Figure 7 left panels) in the case of both, auranofin (malaria and toxoplasmosis) and Bay 11-7085 (toxoplasmosis) represent interesting prospects for future development as antiparasitic agents.

#### 4. Discussion

Emerging drug resistance on the part of *P. falciparum* and *T. gondii* reinforces the urgent need to find new drugs to combat malaria and toxoplasmosis. Importantly in this context, this is the first study to use HTS to identify small molecules that target PfIMP $\alpha$ . In particular, we screened for compounds able to inhibit PfIMP $\alpha$  recognition of a *P. falciparum* NLS (from TGS1, involved in methylation of *P. falciparum* spliceosome RNAs). Through cycles of counter screening, selectivity testing,  $\text{IC}_{50}$  analysis, and antiparasitic testing, it proved possible to identify several small molecules that have the ability to both inhibit PfIMP $\alpha$ :NLS binding, and limit the growth of *P. falciparum* and/or *T. gondii*, as we show here for the first time. Importantly, this study validates IMP $\alpha$ -dependent nuclear protein import as a target for therapeutic intervention in the case of apicomplexan parasites, consistent with the fact that both parasitic organisms have a single, essential IMP $\alpha$  gene [5,33,34].

Of the various hit compounds analyzed, Bay 11-7085 was unique in being a selective inhibitor of PfIMP $\alpha$  (12–16-fold lower  $\text{IC}_{50}$  value), compared to both TgIMP $\alpha$  and MmIMP $\alpha$  in IMP $\alpha$ :NLS binding assays. Further, TSA analysis showed that binding of this compound has differential effects on PfIMP $\alpha$  compared to the other IMP $\alpha$ s; firstly, binding of Bay 11-7085 to PfIMP $\alpha$  increased its thermostability, in contrast to both TgIMP $\alpha$  and MmIMP $\alpha$  where binding decreases thermostability (Figure 4). Further, TSA analysis for Bay 11-7085 indicated a biphasic effect for PfIMP $\alpha$  (Figure 4 left), where lower concentrations appeared to destabilize PfIMP $\alpha$  (in similar fashion to Bay 11-7085's effects throughout on TgIMP $\alpha$  and MmIMP $\alpha$ ; see Figure 4 middle and right), although higher concentrations ( $>20 \mu\text{M}$ ) led to a marked stabilization of the protein. The results imply that Bay 11-7085 likely binds a

site(s) onto the PfIMP $\alpha$  that is distinct to the site(s) it binds onto the TgIMP $\alpha$  and MmIMP $\alpha$  IMP $\alpha$ , consistent with the fact that the amino acid similarity between PfIMP $\alpha$  and TgIMP $\alpha$  and PfIMP $\alpha$  and MmIMP $\alpha$ , respectively, is 54 and 41% (with homology between TgIMP $\alpha$  and MmIMP $\alpha$  43%). The distinct effects of the binding of Bay 11-7085 to PfIMP $\alpha$  are thus likely due to key sequence differences between the various IMP $\alpha$ s. Molecular docking and crystallographic studies of PfIMP $\alpha$  in the absence or presence of Bay 11-7085 should help confirm this, as well as provide more detailed information about the mechanisms of the binding of these small molecules, and help guide future efforts to develop small molecules specifically targeting “hot spot residues” of PfIMP $\alpha$ .

Surprisingly, although Bay 11-7085 appeared to be a selective inhibitor of PfIMP $\alpha$  binding to *P. falciparum* TGS1- NLS in vitro, it was not a potent inhibitor of *P. falciparum* parasites in culture (Figure 5A); in contrast, it exhibited strong inhibition of *T. gondii* tachzoites (Figure 5B; Figure 7 middle panel). This suggests that there may be differences in the uptake and/or catabolism of the compound in the case of *P. falciparum* parasites and *T. gondii* tachzoites, which is a limitation in terms of considering Bay 11-7085 as a potential anti-malarial agent in the future. Bay 11-7085 is a known irreversible inhibitor of Nuclear Factor- $\kappa$ B (NF- $\kappa$ B) [56]; although antiparasitic activity has not previously been reported for Bay 11-7085, a closely related structural analogue Bay 11-7082 has been shown to inhibit the growth of *T. gondii* tachyzoites [49]. This is consistent with the Bay 11-7085/7082 scaffold having inhibitory activity towards *T. gondii*. In fact, as shown here for the first time, Bay 11-7085 can kill *T. gondii* tachyzoites at low  $\mu$ M concentration, with a selectivity index of three; Bay 11-7085 and its structural analogues thus represent a viable starting point for drug development to combat *T. gondii*, and potentially also *P. falciparum*.

In terms of the less selective hit compounds emerging from our screen, auranofin (MMV688978) was the most potent, showing IC<sub>50</sub> values in the nM range for PfIMP $\alpha$ :NLS binding. Auranofin exhibits reactivity for the thiol group of proteins [57] and is a potent inhibitor of thioredoxin reductase enzymes, which may be the basis for its apparent action on IMP $\alpha$  from PfIMP $\alpha$ . TSA analysis implies that auranofin can destabilize (reduce the thermostability of) all three IMP $\alpha$  proteins examined here. Auranofin has previously been shown to possess activity against *P. falciparum* [58], as well as cultured *T. gondii* [59], and we confirm this here for both parasites. Since auranofin is FDA-approved for human use in gold-conjugated form to treat rheumatoid arthritis [57], its apparent effect on apicomplexan IMP $\alpha$  documented here, together with its robust antiparasitic effects against *P. falciparum* and *T. gondii*, indicate its potential for future investigation as an antiparasitic for malaria and toxoplasmosis.

In summary, this is the first HTS to target PfIMP $\alpha$  binding to NLS-containing proteins. The fact that several hit compounds possess antiparasitic activity with low host cell cytotoxicity, validates apicomplexan IMP $\alpha$  as a therapeutic target, and opens the way both for larger screens using strategies similar to those described here, and for future investigation into the candidate hit molecules identified here in terms of the molecular details of the host-pathogen interaction. The latter is a priority for future work in this laboratory.

**Supplementary Materials:** The following are available online at <https://www.mdpi.com/article/10.3390/cells11071201/s1>, Figure S1: Low toxicity of auranofin and Bay 11-7085 in HFF cells. Freshly confluent HFF cells were treated with increasing concentrations of auranofin and Bay 11-7085 as indicated for 48 h followed by an MTT assay, performed as described in the Section 2. Results represent the mean  $\pm$  SD for duplicate wells from a single assay, representative of 2 independent experiments (see Table S1 for pooled data). Table S1: Summary of IC<sub>50</sub>, CC<sub>50</sub> and Selectivity Index data for auranofin and Bay 11-7085 in *T. gondii* tachyzoites/HFF host cells.

**Author Contributions:** Conceptualization: D.A.J., S.P., S.B.W. and K.M.W.; Analysis and performance of experiments: S.B.W. Investigation: S.B.W., D.A.J., S.P. and experiments for HTS at MIPS: S.B.W., M.M.D. and C.H.; TgIMP $\alpha$  construct generation: V.D.; *T. gondii* drug assays: C.K. Funding Acquisition: D.A.J. and S.P.; Supervision: D.A.J., S.P. and K.M.W.; Project administration: D.A.J. and S.P.; Writing original draft: S.B.W.; Writing- review and editing: S.P. and D.A.J. All authors have read and agreed to the published version of the manuscript.

**Funding:** The authors acknowledge the financial support of the National Health and Medical Research Council Australia (Senior Principal Research Fellowship APP1002486/APP1103050) to D.A.J. and Department of Science and Technology (DST), Science and Engineering Research Board (SERB Core Research Grant CRG/2018/000129), India to S.P., S.B.W. acknowledges the support of a Ph.D. scholarship from IITB/Monash University and support from the Department of Biotechnology, India, for project IMURA 0716 to IITB/Monash University.

**Institutional Review Board Statement:** Not applicable.

**Informed Consent Statement:** Not applicable.

**Data Availability Statement:** Not applicable.

**Acknowledgments:** The authors acknowledge MMV (Medicines for Malaria Venture, Switzerland) for providing the Pathogen Box Library used in this research, IIT Bombay Hospital, staff, and volunteers for their help in the blood collection for *P. falciparum* cultures, Patrick Sexton for making available the robotic instruments of the Screening Facility at Monash Institute of Pharmacological Sciences for the HTS, and Sanjeeva Srivastava and Prakriti Tayalia (BSBE, IITB) for the use of plate readers for the parasitic drug assays.

**Conflicts of Interest:** The authors declare no conflict of interest. The funders had no role in the design of the study, in the collection, analyses, or interpretation of data, in the writing of the manuscript, or in the decision to publish the results.

## References

1. Cowman, A.F.; Healer, J.; Marapana, D.; Marsh, K. Malaria: Biology and Disease. *Cell* **2016**, *167*, 610–624. [CrossRef] [PubMed]
2. Furtado, J.M.; Smith, J.R.; Belfort, R.; Gattey, D.; Winthrop, K.L. Toxoplasmosis: A global threat. *J. Glob. Infect. Dis.* **2011**, *3*, 281–284. [CrossRef] [PubMed]
3. World Health Organization. World Malaria Report 2021. Available online: <https://www.who.int/teams/global-malaria-programme/reports/world-malaria-report-2021> (accessed on 29 March 2022).
4. Montazeri, M.; Mehrzadi, S.; Sharif, M.; Sarvi, S.; Tanzifi, A.; Aghayan, S.A.; Daryani, A. Drug Resistance in *Toxoplasma gondii*. *Front. Microbiol.* **2018**, *9*, 2587. [CrossRef] [PubMed]
5. Alday, P.H.; Doggett, J.S. Drugs in Development for Toxoplasmosis: Advances, Challenges, and Current Status. *Drug Des. Dev. Ther.* **2017**, *11*, 273–293. [CrossRef] [PubMed]
6. Dunay, I.R.; Gajurel, K.; Dhakal, R.; Liesenfeld, O.; Montoya, J.G. Treatment of Toxoplasmosis: Historical Perspective, Animal Models, and Current Clinical Practice. *Clin. Microbiol. Rev.* **2018**, *31*, e00057-17. [CrossRef]
7. Konstantinovic, N.; Guegan, H.; Stäjner, T.; Belaz, S.; Robert-Gangneux, F. Treatment of toxoplasmosis: Current options and future perspectives. *Food Waterborne Parasitol.* **2019**, *15*, e00036. [CrossRef] [PubMed]
8. Cui, L.; Mharakurwa, S.; Ndiaye, D.; Rathod, P.K.; Rosenthal, P.J. Antimalarial Drug Resistance: Literature Review and Activities and Findings of the ICEMR Network. *Am. J. Trop. Med. Hyg.* **2015**, *93*, 57–68. [CrossRef] [PubMed]
9. Frankel, M.B.; Knoll, L.J. The Ins and Outs of Nuclear Trafficking: Unusual Aspects in Apicomplexan Parasites. *DNA Cell Biol.* **2009**, *28*, 277–284. [CrossRef] [PubMed]
10. Fu, X.; Liang, C.; Li, F.; Wang, L.; Wu, X.; Lu, A.; Xiao, G.; Zhang, G. The rules and functions of nucleocytoplasmic shuttling proteins. *Int. J. Mol. Sci.* **2018**, *19*, 1445. [CrossRef]
11. Miyamoto, Y.; Yamada, K.; Yoneda, Y. Importin  $\alpha$ : A Key Molecule in Nuclear Transport and Non-Transport Functions. *J. Biochem.* **2016**, *160*, 69–75. [CrossRef]
12. Loveland, K.L.; Major, A.T.; Butler, R.; Young, J.C.; Jans, D.A.; Miyamoto, Y. Putting things in place for fertilization: Discovering roles for importin proteins in cell fate and spermatogenesis. *Asian J. Androl.* **2015**, *17*, 537–544. [CrossRef] [PubMed]
13. Fulcher, A.J.; Jans, D.A. Regulation of Nucleocytoplasmic Trafficking of Viral Proteins: An Integral Role in Pathogenesis? *Biochim. Biophys.* **2011**, *1813*, 2176–2190. [CrossRef]
14. Marfori, M.; Mynott, A.; Ellis, J.J.; Mehdi, A.M.; Saunders, N.F.W.; Curmi, P.M.; Forwood, J.K.; Bodén, M.; Kobe, B. Molecular Basis for Specificity of Nuclear Import and Prediction of Nuclear Localization. *Biochim. Biophys. Acta* **2011**, *1813*, 1562–1577. [CrossRef]
15. Kobe, B. Autoinhibition by an internal nuclear localization signal revealed by the crystal structure of mammalian importin alpha. *Nat. Struct. Biol.* **1999**, *6*, 388–397. [CrossRef] [PubMed]
16. Harreman, M.T.; Hodel, M.R.; Fanara, P.; Hodel, A.E.; Corbett, A.H. The Auto-inhibitory Function of Importin  $\alpha$  Is Essential in Vivo. *J. Biol. Chem.* **2003**, *278*, 5854–5863. [CrossRef] [PubMed]
17. Chahine, M.N.; Pierce, G.N. Therapeutic Targeting of Nuclear Protein Import in Pathological Cell Conditions. *Pharmacol. Rev.* **2009**, *61*, 358–372. [CrossRef] [PubMed]
18. Kosyna, F.; Depping, R. Controlling the Gatekeeper: Therapeutic Targeting of Nuclear Transport. *Cells* **2018**, *7*, 221. [CrossRef] [PubMed]

19. Jans, D.A.; Martin, A.J.; Wagstaff, K.M. Inhibitors of Nuclear Transport. *Curr. Opin. Cell Biol.* **2019**, *58*, 50–60. [[CrossRef](#)] [[PubMed](#)]
20. Martin, A.J.; Jans, D.A. Antivirals That Target the Host IMP $\alpha$ /B1-Virus Interface. *Biochem. Soc. Trans.* **2021**, *49*, 281–295. [[CrossRef](#)]
21. Wagstaff, K.M.; Rawlinson, S.M.; Hearps, A.C.; Jans, D.A. An ALPHAscreen based assay for high-throughput screening for specific inhibitors of nuclear import. *J. Biomol. Screen.* **2011**, *16*, 192–200. [[CrossRef](#)] [[PubMed](#)]
22. Fraser, J.E.; Watanabe, S.; Wang, C.; Chan, W.K.; Maher, B.; Lopez-Denman, A.; Hick, C.; Wagstaff, K.M.; Mackenzie, J.M.; Sexton, P.M.; et al. A nuclear transport inhibitor that modulates the unfolded protein response and provides in vivo protection against lethal dengue virus infection. *J. Infect. Dis.* **2014**, *210*, 1780–1791. [[CrossRef](#)] [[PubMed](#)]
23. Thomas, D.R.; Lundberg, L.; Pinkhan, C.; Shechter, S.; Debono, A.; Baell, J.; Wagstaff, K.M.; Hick, C.A.; Kehn-Hall, K.; Jans, D.A. Identification of novel antivirals inhibiting recognition of Venezuelan equine encephalitis virus capsid protein by the Importin  $\alpha$ / $\beta$ 1 heterodimer through high-throughput screening. *Antivir. Res.* **2018**, *151*, 8–19. [[CrossRef](#)]
24. Shechter, S.; Thomas, D.R.; Lundberg, L.; Pinkham, C.; Lin, S.-C.; Wagstaff, K.M.; Debono, A.; Kehn-Hall, K.; Jans, D.A. Novel inhibitors targeting Venezuelan equine encephalitis virus capsid protein identified using In Silico Structure-Based-Drug-Design. *Sci Rep.* **2017**, *7*, 17705. [[CrossRef](#)] [[PubMed](#)]
25. Caly, L.; Druce, J.D.; Catton, M.G.; Jans, D.A.; Wagstaff, K.M. The FDA-approved Drug Ivermectin inhibits the replication of SARS-CoV-2 in vitro. *Antivir. Res.* **2020**, *178*, 104787. [[CrossRef](#)]
26. Jans, D.A.; Wagstaff, K.M. The Broad Spectrum Host-Directed Agent Ivermectin as an Antiviral for SARS-CoV-2? *Biochem. Biophys. Res. Commun.* **2021**, *538*, 163–172. [[CrossRef](#)] [[PubMed](#)]
27. Wagstaff, K.M.; Sivakumaran, H.; Heaton, S.M.; Harrich, D.; Jans, D.A. Ivermectin is a specific inhibitor of importin  $\alpha$ / $\beta$ -mediated nuclear import able to inhibit replication of HIV-1 and dengue virus. *Biochem. J.* **2012**, *443*, 851–856. [[CrossRef](#)]
28. Yang, S.N.Y.; Atkinson, S.C.; Wang, C.; Lee, A.; Bogoyevitch, M.A.; Borg, N.A.; Jans, D.A. The broad spectrum antiviral ivermectin targets the host nuclear transport importin  $\alpha$ / $\beta$ 1 heterodimer. *Antiviral Res.* **2020**, *177*, 104760. [[CrossRef](#)] [[PubMed](#)]
29. Tay, M.Y.; Fraser, J.E.; Chan, W.K.K.; Moreland, N.J.; Rathore, A.P.; Wang, C.; Vasudevan, S.G.; Jans, D.A. Nuclear localization of dengue virus (DENV) 1-4 non-structural protein 5; protection against all 4 DENV serotypes by the inhibitor Ivermectin. *Antivir. Res.* **2013**, *99*, 301–306. [[CrossRef](#)]
30. Yang, S.N.Y.; Atkinson, S.C.; Fraser, J.E.; Wang, C.; Maher, B.; Roman, N.; Forwood, J.K.; Wagstaff, K.M.; Borg, N.A.; Jans, D.A. Novel Flavivirus Antiviral That Targets The Host Nuclear Transport Importin  $\alpha$ / $\beta$ 1 Heterodimer. *Cells* **2019**, *8*, 281. [[CrossRef](#)] [[PubMed](#)]
31. Caly, L.; Wagstaff, K.M.; Jans, D.A. Subcellular trafficking of pathogens: Targeting for therapeutics. *Antiviral Res.* **2012**, *95*, 202–206. [[CrossRef](#)] [[PubMed](#)]
32. Seeber, F.; Steinfelder, S. Recent Advances in Understanding Apicomplexan Parasites. *F1000Research* **2016**, *5*, 1–14. [[CrossRef](#)] [[PubMed](#)]
33. Zhang, M.; Wang, C.; Otto, T.D.; Oberstaller, J.; Liao, X.; Adapa, S.R.; Udenze, K.; Bronner, I.F.; Casandra, D.; Mayho, M.; et al. Uncovering the Essential Genes of the Human Malaria Parasite *Plasmodium falciparum* by Saturation Mutagenesis. *Science* **2018**, *360*, 360. [[CrossRef](#)] [[PubMed](#)]
34. Sidik, S.M.; Hackett, C.G.; Tran, F.; Westwood, N.J.; Lourido, S. Efficient Genome Engineering of *Toxoplasma gondii* Using CRISPR/Cas9. *PLoS ONE* **2014**, *9*, e100450. [[CrossRef](#)]
35. Bawankar, P.; Shaw, P.J.; Sardana, R.; Babar, P.H.; Patankar, S. 5' and 3' End Modifications of Spliceosomal RNAs in *Plasmodium falciparum*. *Mol. Biol. Rep.* **2010**, *37*, 2125–2133. [[CrossRef](#)]
36. Babar, P.H.; Dey, V.; Jaiswar, P.; Patankar, S. An Insertion in the Methyltransferase Domain of *P. Falciparum* Trimethylguanosine Synthase Harbors a Classical Nuclear Localization Signal. *Mol. Biochem. Parasitol.* **2016**, *210*, 58–70. [[CrossRef](#)]
37. Dey, V.; Patankar, S. Molecular Basis for the Lack of Auto-Inhibition of *Plasmodium falciparum* Importin  $\alpha$ . *Biochem. Biophys. Res. Commun.* **2018**, *503*, 1792–1797. [[CrossRef](#)]
38. Wagstaff, K.M.; Jans, D.A. Intramolecular Masking of Nuclear Localization Signals: Analysis of Importin Binding Using a Novel AlphaScreen-Based Method. *Anal. Biochem.* **2006**, *348*, 49–56. [[CrossRef](#)]
39. Trager, W.; Jensen, J.B. Human Malaria Parasites in Continuous Culture. *Science* **1976**, *193*, 673–675. [[CrossRef](#)] [[PubMed](#)]
40. Noedl, H.; Wernsdorfer, W.H.; Miller, R.S.; Wongsrichanalai, C. Histidine-Rich Protein II: A Novel Approach to Malaria Drug Sensitivity Testing. *Antimicrob. Agents Chemother.* **2002**, *46*, 1658–1664. [[CrossRef](#)] [[PubMed](#)]
41. Noedl, H.; Bronnert, J.; Yingyuen, K.; Attlmayr, B.; Kollaritsch, H.; Fukuda, M. Simple Histidine-Rich Protein 2 Double-Site Sandwich Enzyme-Linked Immunosorbent Assay for Use in Malaria Drug Sensitivity Testing. *Antimicrob. Agents Chemother.* **2005**, *49*, 3575–3577. [[CrossRef](#)] [[PubMed](#)]
42. Van Dooren, G.G.; Tomova, C.; Agrawal, S.; Humbel, B.M.; Striepen, B. Toxoplasma Gondii Tic20 Is Essential for Apicoplast Protein Import. *Proc. Natl. Acad. Sci. USA* **2008**, *105*, 13574–13579. [[CrossRef](#)] [[PubMed](#)]
43. Sabin, A.B. Toxoplasmic encephalitis in children. *J. Am. Med. Assoc.* **1941**, *116*, 801–807. [[CrossRef](#)]
44. Hughes, H.P.A.; Hudson, L.; Fleck, D.G. In Vitro Culture of *Toxoplasma Gondii* in Primary and Established Cell Lines. *Int. J. Parasitol.* **1986**, *16*, 317–322. [[CrossRef](#)]
45. Black, M.; Seeber, F.; Soldati, D.; Kim, K.; Boothroyd, J.C. Restriction Enzyme-Mediated Integration Elevates Transformation Frequency and Enables Co-Transfection of *Toxoplasma Gondii*. *Mol. Biochem. Parasitol.* **1995**, *74*, 55–63. [[CrossRef](#)]
46. Gubbels, M.J.; Striepen, B. Studying the Cell Biology of Apicomplexan Parasites Using Fluorescent Proteins. *Microsc. Microanal.* **2004**, *10*, 568–579. [[CrossRef](#)] [[PubMed](#)]

47. Jacot, D.; Meissner, M.; Sheiner, L.; Soldati-Favre, D.; Striepen, B. Genetic Manipulation of *Toxoplasma Gondii*. In *Toxoplasma Gondii*; Weiss, L.M., Kim, K., Eds.; Elsevier Academic Press: Burlington, NJ, USA, 2014; pp. 577–611.
48. Striepen, B.; Soldati, D. 15—Genetic Manipulation of *Toxoplasma gondii*. In *Toxoplasma Gondii*; Louis, M., Weiss, L.M., Kim, K., Eds.; Academic Press: Cambridge, MA, USA, 2007; pp. 391–418.
49. Han, Y.; Adeyemi, O.S.; Hazzaz, M.; Kabir, B.; Kato, K. Screening of Compound Libraries for Inhibitors of *Toxoplasma* Growth and Invasion. *Parasitol. Res.* **2020**, *119*, 1675–1681. [[CrossRef](#)] [[PubMed](#)]
50. Subramanian, G.; Belekara, M.A.; Shukla, A.; Tong, J.X.; Sinha, A.; Chu, T.T.T.; Kulkarni, A.S.; Preiser, P.R.; Reddy, D.S.; Tan, K.S.W.; et al. Targeted Phenotypic Screening in *Plasmodium falciparum* and *Toxoplasma gondii* Reveals Novel Modes of Action of Medicines for Malaria Venture Malaria Box Molecules. *mSphere* **2018**, *3*, e00534-17. [[CrossRef](#)]
51. Riss, T.L.; Moravec, R.A.; Niles, A.L.; Duellman, S.; Benink, H.A.; Worzella, T.J.; Minor, L. Cell Viability Assays. In *Assay Guidance Manual*; Markossian, S., Grossman, A., Brimacombe, K., Arkin, M., Auld, D., Christopher, P., Austin, Jonathan, B., Thomas, D.Y., Chung, et al., Eds.; Eli Lilly & Company and the National Center for Advancing Translational Sciences: Bethesda, MD, USA, 2004.
52. Zhang, J.H.; Chung, T.D.; Oldenburg, K.R. A Simple Statistical Parameter for Use in Evaluation and Validation of High Throughput Screening Assays. *J. Biomol. Screen.* **1999**, *4*, 67–73. [[CrossRef](#)]
53. Kurth, F.; Pongratz, P.; B  lard, S.; Mordm  ller, B.; Kremsner, P.G.; Ramharter, M. In Vitro Activity of Pyronaridine against *Plasmodium falciparum* and Comparative Evaluation of Anti-Malarial Drug Susceptibility Assays. *Malar. J.* **2009**, *8*, 79. [[CrossRef](#)]
54. Van der Ven, A.J.A.M.; Schoondermark-van de Ven, E.M.E.; Camps, W.; Melchers, W.J.G.; Koopmans, P.P.; van der Meer, J.W.M.; Galama, J.M.D. Anti-Toxoplasma Effect of Pyrimethamine, Trimethoprim and Sulphonamides Alone and in Combination: Implications for Therapy. *J. Antimicrob. Chemother.* **1996**, *38*, 75–80. [[CrossRef](#)]
55. Baudy, A.R.; Saxena, N.; Gordish, H.; Hoffman, E.P.; Nagaraju, K. A Robust In Vitro Screening Assay to Identify NF-KB Inhibitors for Inflammatory Muscle Diseases. *Int. Immunopharmacol.* **2009**, *9*, 1209–1214. [[CrossRef](#)] [[PubMed](#)]
56. Berger, N.; Ben Bassat, H.; Klein, B.Y.; Laskov, R. Cytotoxicity of NF-KB Inhibitors Bay 11-7085 and Caffeic Acid Phenethyl Ester to Ramos and Other Human B-Lymphoma Cell Lines. *Exper. Hematol.* **2007**, *35*, 1495–1509. [[CrossRef](#)] [[PubMed](#)]
57. Roder, C.; Thomson, M.J. Auranofin: Repurposing an Old Drug for a Golden New Age. *Drugs R D* **2015**, *15*, 13–20. [[CrossRef](#)] [[PubMed](#)]
58. Sannella, A.R.; Casini, A.; Gabbiani, C.; Messori, L.; Bilia, A.R.; Vincieri, F.F.; Majori, G.; Severini, C. New Uses for Old Drugs. Auranofin, a Clinically Established Antiarthritic Metallodrug, Exhibits Potent Antimalarial Effects In Vitro: Mechanistic and Pharmacological Implications. *FEBS Lett.* **2008**, *582*, 844–847. [[CrossRef](#)] [[PubMed](#)]
59. Andrade, R.M.; Chaparro, J.D.; Capparelli, E.; Reed, S.L. Auranofin Is Highly Efficacious against *Toxoplasma gondii* In Vitro and in an In Vivo Experimental Model of Acute Toxoplasmosis. *PLoS Negl. Trop. Dis.* **2014**, *8*, e2973. [[CrossRef](#)] [[PubMed](#)]